Investigation of Early Events in FcεRI-Mediated Signaling Using a Detailed Mathematical Model[1]

James R. Faeder,* William S. Hlavacek,* Ilona Reischl,[2‡] Michael L. Blinov,* Henry Metzger,[‡] Antonio Redondo,[†] Carla Wofsy,*[§] and Byron Goldstein[3]*

Aggregation of FcεRI on mast cells and basophils leads to autophosphorylation and increased activity of the cytosolic protein tyrosine kinase Syk. We investigated the roles of the Src kinase Lyn, the immunoreceptor tyrosine-based activation motifs (ITAMs) on the β and γ subunits of FcεRI, and Syk itself in the activation of Syk. Our approach was to build a detailed mathematical model of reactions involving FcεRI, Lyn, Syk, and a bivalent ligand that aggregates FcεRI. We applied the model to experiments in which covalently cross-linked IgE dimers stimulate rat basophilic leukemia cells. The model makes it possible to test the consistency of mechanistic assumptions with data that alone provide limited mechanistic insight. For example, the model helps sort out mechanisms that jointly control dephosphorylation of receptor subunits. In addition, interpreted in the context of the model, experimentally observed differences between the β- and γ-chains with respect to levels of phosphorylation and rates of dephosphorylation indicate that most cellular Syk, but only a small fraction of Lyn, is available to interact with receptors. We also show that although the β ITAM acts to amplify signaling in experimental systems where its role has been investigated, there are conditions under which the β ITAM will act as an inhibitor. ***The Journal of Immunology*****, 2003, 170: 3769–3781.**

There is increasing recognition that mathematical modeling can be a valuable interpretive and predictive tool for understanding cell signaling cascades (1, 2). In the case of the signaling cascade initiated by the aggregation of FcεRI, the high affinity receptor for IgE, detailed molecular level models have been used to characterize the role of Lyn kinase in the initiation and regulation of FcεRI tyrosine phosphorylation (3, 4). We have recently extended these earlier models to investigate the separate roles of the receptor subunits and the kinases Lyn and Syk in the phosphorylation and activation of Syk (5). Here we provide a detailed description of the model and improved estimates of parameters based on direct experimental measurements and comparison of model predictions with both new and previously reported experimental data.

FcεRI is a member of the family of multichain immune recognition receptors (MIRR),[4] which also includes the B cell Ag receptor (BCR) and TCR (6). The subunits of the MIRR can be divided into those that participate in binding of ligand and those that participate in signaling. All the signaling subunits, but none of the binding subunits, have at least one copy of a common sequence in their cytoplasmic domains called an immunoreceptor tyrosine-based activation motif (ITAM) (7, 8). The earliest cellular response in MIRR-mediated signal transduction is the phosphorylation of ITAM tyrosines by Src family protein tyrosine kinases (PTKs). A member of a second PTK family (Syk in the case of FcεRI and the BCR, and predominantly Zap70 in the case of the TCR) can then bind to doubly phosphorylated ITAMs, become phosphorylated, and mediate additional signaling events.

We model the tetrameric form of FcεRI, which has an α-chain that binds IgE and three ITAM-containing subunits, a β-chain, and two disulfide-linked γ-chains. The tetrameric receptor is the only form found in rodent cells and is also expressed on human basophils and mast cells (9). Human basophils and mast cells also express a trimeric form of the receptor that is missing the β subunit, and other human cell types express only the trimeric form (9).

The unphosphorylated β-chain associates weakly with the Src family kinase Lyn, which is anchored to the inner layer of the plasma membrane (10–14). Upon receptor aggregation, Lyn transphosphorylates tyrosines in the β and γ ITAMs (15, 16). There is a much stronger association of Lyn through its Src homology 2 (SH2) domain with the phosphorylated β ITAM (11, 15). The cytosolic PTK Syk binds with high affinity, through its two SH2 domains to the doubly phosphorylated γ ITAM (17, 18). Syk is phosphorylated on multiple tyrosines by both Lyn and Syk (19–23), with Syk playing the major role in phosphorylating the two tyrosines, 519 and 520, in the Syk activation loop (24, 25). This yields a fully activated Syk that is required for calcium mobilization (22, 24, 25).

The model that we present describes association, dissociation, and phosphorylation reactions among four components: the receptor FcεRI, a bivalent ligand that aggregates receptors into dimers, and the PTKs, Lyn and Syk. The model also includes dephosphorylation reactions mediated by a pool of protein tyrosine phosphatases. Even with simplifying assumptions, justified below based on experimental considerations, the reactions among the components

*Theoretical Biology and Biophysics Group and [†]Theoretical Chemistry and Molecular Physics Group, Theoretical Division, Los Alamos National Laboratory, Los Alamos, NM 87545; [‡]Arthritis and Rheumatism Branch, National Institute of Arthritis and Musculoskeletal and Skin Diseases, National Institutes of Health, Bethesda, MD 20892; and [§]Department of Mathematics and Statistics, University of New Mexico, Albuquerque, NM 87131

Received for publication December 4, 2002. Accepted for publication January 28, 2003.

The costs of publication of this article were defrayed in part by the payment of page charges. This article must therefore be hereby marked *advertisement* in accordance with 18 U.S.C. Section 1734 solely to indicate this fact.

[1] This work was supported by National Institutes of Health Grant GM35556 and the U.S. Department of Energy under Contract W-7405-ENG-36 through the Los Alamos National Laboratory LDRD program.

[2] Current address: U.S. Food and Drug Administration, Center for Biologics Evaluation and Research, HFM-564, Bethesda, MD 20892-4555.

[3] Address correspondence and reprint requests to Dr. Byron Goldstein, Theoretical Biology and Biophysics Group, MS K710, Theoretical Division, Los Alamos National Laboratory, Los Alamos, NM 87545. E-mail address: bxg@lanl.gov

[4] Abbreviations used in this paper: MIRR, multichain immune recognition receptor; ITAM, immunoreceptor tyrosine-based activation motif; PTK, protein tyrosine kinase; RBL, rat basophilic leukemia; SH2, Src homology; BCR, B cell Ag receptor.

0022-1767/03/$02.00

generate a network of 354 distinct molecular species. The model predicts levels of association and phosphorylation of molecular complexes as they vary with time, ligand concentration, concentrations of signaling components, or genetic modifications of the interacting proteins. Therefore, the model can be used to analyze a wide variety of experimental data, and the data provide multiple tests of the model. We estimate parameters for rat basophilic leukemia (RBL) cells stimulated by covalently cross-linked IgE dimers (26–28).

The model survives a stringent test. For experiments that carry information relevant to the experimental system under consideration and that are expected to reflect only the molecules in the model, we identify a set of reaction rate constants for which model predictions are consistent, quantitatively, with published data and with additional experiments that we report here.

The analysis we present offers new information about the factors that control receptor dephosphorylation, access of receptors to Lyn and Syk, and the role of the phosphorylated β ITAM. We find that intrinsic rates of ITAM dephosphorylation are orders of magnitude faster than the apparent rates measured experimentally. SH2 domains bound to phosphotyrosines protect the sites they are bound to from dephosphorylation (29). Because SH2-bound Lyn and Syk protect phosphorylated sites from dephosphorylation, observed time courses of ITAM dephosphorylation reflect, along with intrinsic phosphatase activity, the amounts of Lyn and Syk available to bind, through their SH2 domains, to phosphorylated ITAMs and the rate constants for binding and dissociation. The amount of phosphorylation of the γ ITAM relative to the β ITAM is another important point of contact between model and experiment, where model predictions differ sharply depending on the amount of Syk available to interact with FcεRI. For the model to be consistent with the data, much more Syk than Lyn must be available. The model also shows that the β ITAM may act as a strong or a weak amplifier of signaling or even as a weak inhibitor, depending on the rate at which Lyn transphosphorylates the γ ITAM. Parameter estimates presented here reflect experimental evidence that the β ITAM functions as an amplifier (30).

Materials and Methods

Cell lysates and immunoprecipitation

RBL-2H3 cells were harvested with trypsin-EDTA, washed in buffer A (150 mM NaCl, 5 mM KCl, 5.4 mM glucose, 1.8 mM $CaCl_2$, 1 mM $MgCl_2$, and 25 mM PIPES, pH 7.2, containing 0.1% BSA), and resuspended in buffer A at 1.5×10^7 cells/ml. Cells were reacted with different doses of either monomeric or chemically cross-linked dimers of mouse IgE (28) for 10 min before cell lysis in 0.5 vol of ice-cold 3× solubilization buffer (pH 7.6) to yield a final concentration of 0.17% Triton X-100, 50 mM Tris, 50 mM NaCl, 5 mM EDTA, 1 mM Na_3VO_4, 5 mM $Na_4P_2O_7$, 50 mM NaF, 2 mM iodoacetate, 1 mM PMSF, and 10 μg/ml each of aprotinin, leupeptin, and pepstatin A and agitated for 30 min at 4°C. After 5 min of centrifugation, target proteins were immunoprecipitated from the supernatant with shaking for 3 h at 4°C. IgE-bound FcεRI was precipitated with goat anti-mouse IgE Abs (ICN Biomedicals, Aurora, OH) using protein A-Sepharose beads (Amersham Pharmacia Biotech, Piscataway, NJ). Phosphorylated proteins were precipitated with mAb 4G10 (Upstate Biotechnologies, Lake Placid, NY) using protein G-Sepharose beads (Amersham Pharmacia Biotech). Syk was precipitated using scFv G4G11 (31) prebound overnight to anti-Myc beads (clone 9E10; Covance, Richmond, CA).

Western blot

Samples were run on 8 or 12% Tris-glycine gels (Invitrogen, Carlsbad, CA) followed by semidry transfer to Protran nitrocellulose membranes (Schleicher & Schuell, Dassel, Germany). Following a blocking step (32, 33), phosphorylated proteins were detected with 4G10-biotin (Upstate Biotechnologies) and NeutrAvidin-HRP (Pierce, Rockford, IL). The FcεRI β-chain was detected with Ab JRK (34), and Syk was detected with a monoclonal anti-Syk, Syk01/Pr (35), both followed by HRP-conjugated sheep-anti-mouse $F(ab)_2$ (Sigma-Aldrich, St. Louis, MO), ECL, and exposure of Hyperfilm ECL (both from Amersham Pharmacia Biotech). Stripping of membranes was performed with Restore Western Blot Stripping buffer (Pierce) for 15 min at room temperature, followed by two 10-min washes in TTBS (50 mM Tris, 150 mM NaCl, and 0.05% (v/v) Tween 20, adjusted to pH 7.5 with HCl).

Quantification of Syk protein

Syk SH2-GST fusion protein was produced and purified as previously described (36) and was used to generate a calibration curve. The construct, with 492 residues total, consists of a 24-aa leader sequence, residues 10–261 from human Syk, and GST from *Schistosoma japonicum*; has a M_r of 56.4 kDa, and has a molar extinction coefficient of 78,489 cm^{-1} M^{-1} (37). A stock solution (OD, 0.09) was diluted in siliconized tubes in buffer A (150 mM NaCl, 5 mM KCl, 25 mM PIPES, 5.4 mM glucose, 1 mM $MgCl_2$, 1.8 mM $CaCl_2$, and 0.1% BSA, adjusted to pH 7.2) and run on the same gel, either separately or mixed with lysate of RBL cells. The relative amounts of the construct and the endogenous protein were determined by quantitating the amount of bound anti-Syk Ab, directed against the SH2 domains of Syk (38) by densitometric evaluation of Western blots. The average number of Syk molecules per RBL cell based on 15 measurements from four experiments was calculated from the calibration curve.

Mathematical Model

The model is based on the following sequence of early events in signaling through the FcεRI (39, 40): ligand-receptor binding leading to aggregation of receptors at the plasma membrane, transphosphorylation of specific tyrosine residues in the ITAMs of aggregated receptors by constitutively associated Lyn kinase, recruitment of additional Lyn and of Syk kinase to the phosphorylated ITAMs, and subsequent transphosphorylation of Syk by both Lyn and Syk. The full activation of Syk through the phosphorylation of two adjacent tyrosine residues in the activation loop of its kinase domain is required for downstream events, including calcium mobilization and degranulation (24). Although these events are typically described as a linear sequence of chemical reactions, the early signaling events form a highly branched chemical network involving a large number of different chemical species.

The model was constructed in the following steps, which can serve as a general template for the development of signaling models: 1) identify components and their interactions to generate a set of feasible chemical species that participate in the signaling process being studied, 2) develop reaction rules for these species to construct a chemical network, 3) determine values of reaction rate constants and initial concentrations based on direct measurements and other experimental observations, 4) convert the network into a predictive mathematical model consisting of a set of coupled differential equations, 5) solve the equations numerically to obtain predictions for a given set of initial conditions, and 6) modify the values of specific parameters as necessary to improve agreement between the predictions of the model and experimental observations. Although our model is specific to FcεRI-mediated signaling, it can be adapted to other signaling pathways that share a similar sequence of initial events, e.g., B cell receptor signaling, and it can be extended to include additional signaling molecules, such as coreceptors, specific phosphatases, and solution- and surface-associated adapters.

Components

The tetrameric FcεRI is modeled as three subunits, with the disulfide-bonded pair of γ-chains treated as one unit (Fig. 1*a*). The extracellular region of the α-chain binds to the Fc portion of IgE. The ligand shown here is a covalently cross-linked dimer of IgE (26), which can induce receptor phosphorylation and degranulation of RBL cells and is convenient because it forms only dimer receptor aggregates, and its kinetics have been well characterized (28). The model can be applied, however, to any situation where

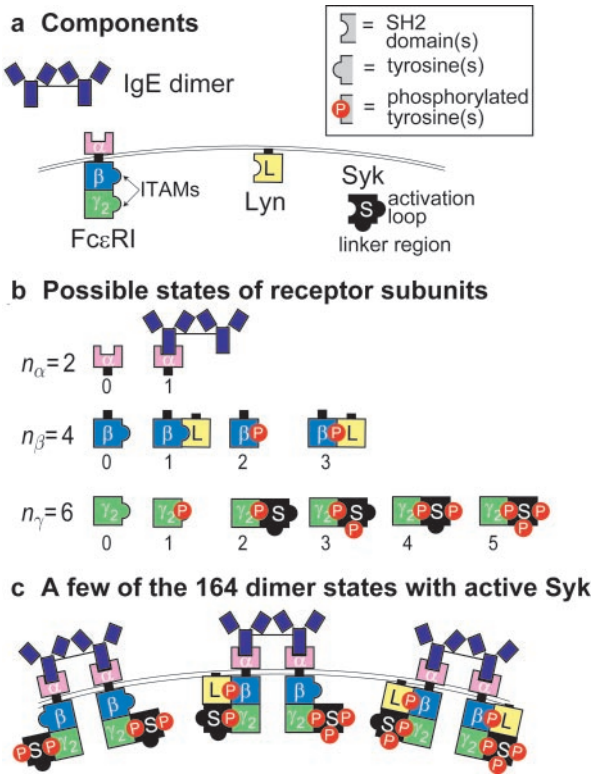

FIGURE 1. Model for the early events in FcεRI signaling induced by a bivalent ligand: representation of molecular components and states. *a*, The bivalent ligand shown is a covalently cross-linked IgE dimer. The tetrameric form of FcεRI, the high affinity receptor for IgE, consists of an α subunit that binds IgE, a β subunit, and a disulfide-linked dimer of γ subunits. The β and γ subunits contain ITAMs that become phosphorylated on tyrosine residues. The membrane-associated kinase Lyn can associate with the unphosphorylated or phosphorylated β subunit. The cytosolic kinase Syk associates with a doubly phosphorylated γ ITAM. On the representations of the kinases, notches indicate SH2 domains. The tandem SH2 domains of Syk are lumped together in the representation. On β, γ, and Syk, bumps represent groups of tyrosines that are lumped in the model as single targets for phosphorylation. On Syk, the model distinguishes tyrosines in the linker region, which are phosphorylated by Lyn, and those in the activation loop, which are phosphorylated by Syk. *b*, The α subunit can be bound to ligand or unbound (two states of α). The β subunit can be unphosphorylated or phosphorylated, with or without associated Lyn (four states of β). The γ dimer can be unphosphorylated or phosphorylated, and the phosphorylated form can be bound to Syk in any of four states of phosphorylation (six states of γ). *c*, There are 300 possible states for cross-linked FcεRI dimers, of which 164 contain autophosphorylated Syk. Three of these states containing active Syk are shown.

the ligand is bivalent and the receptor is effectively monovalent, as would be the case if bispecific IgE were used to sensitize the cells (41). In this case the high affinity IgE molecule would be considered part of the binding subunit of the receptor.

The β subunit and the γ dimer contain the ITAMs that, upon phosphorylation, become binding sites for the SH2 domains of the two kinases, Lyn and Syk. The major simplification we make in the model is that multiple tyrosine residues on receptor subunits and Syk are treated as single units of phosphorylation, as indicated in Fig. 1. For example, the β ITAM contains three tyrosines, but in the model the ITAM is either phosphorylated or not phosphorylated. Sites of Syk tyrosine phosphorylation are lumped into two units: the activation loop, which is phosphorylated by Syk, and the linker region, which is phosphorylated by Lyn.

Fig. 1*b* shows the states of the β-chain and the γ dimer included in the model. Each unit can be phosphorylated or unphosphorylated, and can be associated with a kinase in any of several states. In the model, each β-chain and γ dimer can bind only a single kinase molecule at a time. The actual stoichiometry of Syk binding to the γ dimer is unknown. The assumption that only one Syk binds to a γ dimer seems reasonable given the size disparity between the cytoplasmic domain of each γ chain (4.5 kDa) and Syk (72 kDa). Modifying the model to allow two Syk molecules to bind to the two chains in a γ dimer would increase the complexity of the model, but such complexity can be accommodated if the stoichiometry is determined to be 2.

The model permits a large number of receptor states (Fig. 1, *b* and *c*). Since the state of each subunit is independent of the states of the other subunits, the total number of monomer states is $n_\alpha n_\beta n_\gamma = 48$. In a dimer, each α subunit must be engaged with the ligand, so the total number of dimer states is $n_\beta n_\gamma(n_\beta n_\gamma + 1)/2 = 300$. In addition, there are six nonreceptor states, free ligand, free Lyn, and Syk in each of its four possible states of phosphorylation, to give a total of 354 distinct chemical species in the model.

Reaction classes

The signaling model is composed of the 354 chemical species we have just described and the chemical reactions that connect them. The reaction network is constructed using a set of reaction rules or classes, each of which describes the formation and breaking of a chemical interaction based only on the presence of specific motifs in the chemical species involved. For example, as illustrated in Fig. 2, there are only two classes of reaction to describe the formation of a ligand-receptor bond depending only on whether one Fc region of the IgE dimer is already bound to the receptor. There is experimental evidence that the ligand-receptor interactions in this system are unaffected by modifications of the cytoplasmic portion of the receptor (33). Therefore, we assume that rate constants for binding reactions are independent of the states of β and γ subunits. As a result, only two rate constants parameterize the 48 reactions (considering forward and reverse reactions separately) for binding of free IgE dimer to FcεRI. Similarly, only two rate constants parameterize the far greater number of aggregation reactions (1152), where a free receptor binds to an IgE dimer that is already bound to a receptor. In the current model, 15 reaction classes and 21 rate constants are used to describe the 3680 chemical transformations that can occur. In this way the limited experimental information about the kinetics of signaling reactions can be combined with the much larger amount of information about the structure of the components and the interactions among them.

Each reaction class is represented in Fig. 2 by its simplest member, i.e., the reactants shown have the minimal set of modifications required to carry out the given reaction. The full list of 3680 possible reactions is generated by a computer algorithm that, for each reaction class, checks each of the chemical species to determine whether it can participate in a reaction in that class. For example, a dimer with no associated Lyn or Syk cannot participate in a phosphorylation reaction, but can participate in some other classes of reactions, for example, the constitutive association of Lyn. The rate of each reaction is simply the product of the rate constant and each of the reactant concentrations (elementary reaction kinetics). The rate of change of each species involved in a reaction is increased by this rate for product species and decreased by this rate for reactant species.

Network structure and parameters

We will now describe the reaction events and associated parameters in more detail. The reaction model requires as input not only

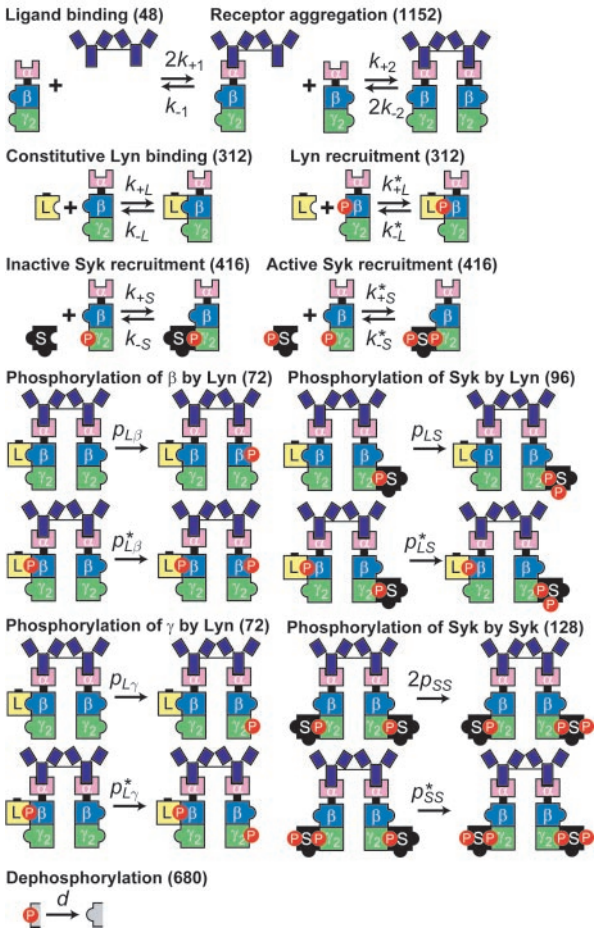

FIGURE 2. The 15 reaction classes and 21 rate constants in the model. The number of reactions contained in each class (counting forward and reverse reactions separately) is listed in parentheses.

the rate constants associated with each of the reactions, but also the initial concentrations of each of the components, which are specific to the cell type being modeled. In this work we have chosen parameters appropriate to the RBL cell to facilitate comparison between the simulation results and experiments. A summary of the parameters is given in Table I.

The reactions that describe ligand-receptor binding and ligand-induced receptor aggregation have been used previously to model the binding kinetics of the ^{125}I-labeled IgE dimers to RBL cells (28). The four rate constants determined by a fit to the experimental data in that work are given in Table I. We have set the reverse rate constants to zero in the simulations, which has a negligible effect on time scales under a few hours, but facilitates checking the numerical results for convergence. We estimate that there are $\sim 4 \times 10^5$ FcεRI/cell for the RBL cells used in the current study.

The model permits Lyn to associate with the receptor in two ways. Lyn associates weakly with the unphosphorylated receptor (10–12) through an interaction between its unique domain and the C-terminal cytoplasmic tail of the β subunit (13, 14). This association is denoted in Fig. 2 as constitutive Lyn binding. Upon phosphorylation of the β ITAM, Lyn is recruited with much higher affinity through its SH2 domain (11, 15, 42). These reactions and their associated parameters are based on our earlier model of Lyn activity that did not include Syk (3). The amount of Lyn available to bind receptors was fit to receptor phosphorylation kinetics and was determined to be ~7% of the number of FcεRI (3). Although this number is far lower than the actual number of Lyn molecules typically measured in RBL cells, several competition experiments (43, 44) have demonstrated that Lyn kinase is available in limiting concentrations in RBL cells. The equilibrium constant for the constitutive interaction was based on the results of chemical cross-linking experiments that indicated that ~3–4% of receptors in resting RBL cells were associated with Lyn (11). Finally, the equilibrium constant for the high affinity interaction was estimated from equilibrium constants of similar SH2-phosphopeptide interactions measured in solution (3). The four rate constants for Lyn association are determined by the two equilibrium constants, the assumption that the forward rate constant is identical for both forms of association, and a fit of the model to β ITAM dephosphorylation data, as described below. As a result of this fitting, we estimate that the rate constant for dissociation of Lyn from the phosphorylated ITAM, k^*_{-L}, is about an order of magnitude faster than previously estimated (3).

Syk associates with FcεRI primarily through an interaction between its tandem SH2 domains and the doubly phosphorylated γ ITAM (36, 42, 45, 46). Syk has at least a 1000-fold lower affinity for the singly phosphorylated γ ITAM peptide (36) and at least a 20-fold lower affinity for the doubly phosphorylated β ITAM (46). The equilibrium dissociation constant, K_d, for the interaction of Syk's tandem SH2 domains with the diphosphorylated γ ITAM peptide sequence has been determined with both surface plasmon resonance (46) and a scintillation proximity assay (36) at 25°C, and comparable results were obtained. We use a value of 2.6 nM for K_d in the current model. The only two measured values for the dissociation of Syk's tandem SH2 domains from a diphosphorylated ITAM peptide are 0.01 s^{-1} (36) and 0.7 s^{-1} (47) at 25°C. In addition, Grucza et al. (47) have observed a very strong temperature dependence of binding in the range 25–37°C, which they attributed to a conformational change in Syk. The dissociation rate constant in our model is obtained from a fit of model predictions to the observed rate of γ ITAM dephosphorylation, as described below, and is intermediate between the measured values. It is also very similar to the rate constant we estimate for Lyn dissociation from the phosphorylated β ITAM. In the current parameter set, the Syk dissociation rate constant does not change when Syk is phosphorylated (20, 21), although the structure of the model permits such a distinction if subsequent evidence shows that this regulatory mechanism is important in FcεRI-mediated pathways. We estimate that $\sim 3.4 \times 10^5$ Syk molecules/cell are present in the RBL cells used in the current study. In contrast with Lyn kinase, the analysis presented below indicates that all or most of the Syk is available to interact with receptors.

Lyn associated with a receptor aggregate can transphosphorylate both the β and γ ITAMs (15) and Syk associated with an adjacent receptor (19, 21). As in our previous model of FcεRI-mediated Lyn activity (3), it is assumed that all available Lyn is in a form that, when associated with an aggregated receptor, can initiate transphosphorylation. We do not address the issues of how the size of the pool of available Lyn or the activity of Lyn is regulated. The model is consistent with the finding that a single Lyn molecule in an aggregate is sufficient to induce receptor phosphorylation (4), which demonstrates that Lyn clustering and Lyn-Lyn transphosphorylation within receptor aggregates are not required for Lyn activity. In general, the results of the model are not sensitive to the absolute rates of phosphorylation, which are chosen simply to ensure that most of the Lyn that is SH2-bound to receptor aggregates produces phosphorylation, i.e., phosphorylation is faster than dephosphorylation. In the current parameter set the dephosphorylation rate constant is 20 s^{-1} (see *Interpretation of dephosphorylation kinetics*); therefore, the rate constant for β phosphorylation by SH2-bound Lyn ($p^*_{L\beta}$) was taken to be 100 s^{-1}. Relative rates of

Table I. *Model parameter values*[a]

Parameter	Value	Reference
Components[b]		
Receptors, R_T	4×10^5/cell	Current work
Lyn, L_T	2.8×10^4/cell	Available Lyn $\sim 0.07 \times R_T$ (3)
Syk, S_T	4×10^5/cell	Current work[c]
Ligand binding		
k_{+1}	1.3×10^{-10} molecules^{-1} s^{-1} (8×10^4 M^{-1} s^{-1})	Estimated binding parameters for covalently cross-linked IgE dimer (3)
k_{+2}	2.5×10^{-4} molecules^{-1} s^{-1}	$k_{+2}R_T = 100$ s^{-1} (3)
k_{-1}, k_{-2}	0	10^{-5} s$^{-1} \sim 0$ over reported time scales
Lyn association		
k_{+L}, k_{+L}	5×10^{-5} molecules^{-1} s^{-1}	Based on estimated equilibrium constants in Ref. 3
k_{-L}	20 s^{-1}	Based on estimated equilibrium constants in Ref. 3
k^*_{-L}	0.12 s^{-1}	Fit to observed rate of β ITAM dephosphorylation from Ref. 51
Syk association		
k_{+S}, k^*_{+S}	6×10^{-5} molecules^{-1} s^{-1}	Based on measured equilibrium constant at 25°C for binding of Syk tandem SH2 domains (46)
k_{-S}, k^*_{-S}	0.13 s^{-1}	Fit to observed rate of γ ITAM dephosphorylation in Ref. 51
Phosphorylation		
$p_{L\beta}$, p_{LS}	30 s^{-1}	Consistent with extensive receptor phosphorylation
$p^*_{L\beta}$, p^*_{LS}	100 s^{-1}	Moderate increase in Lyn kinase activity upon SH2 domain binding (15)
$p_{L\gamma}$	1 s^{-1}	Double phosphorylation of γ ITAM tyrosine, required to bind Syk, slower than single phosphorylation (48, 49, 77)
$p^*_{L\gamma}$	3 s^{-1}	Moderate increase in Lyn kinase activity upon SH2 domain binding (15)
p_{SS}	100 s^{-1}	Assumed same kinase activity as recruited Lyn
p^*_{SS}	200 s^{-1}	Moderate increase in Syk kinase activity upon phosphorylation of the activation loop (24)
Dephosphorylation		
d	20 s^{-1}	Fit to rates of ITAM dephosphorylation in Ref. 51

[a] Reactions associated with these rate constants are shown in Fig. 2.
[b] Cell density assumed to be 1×10^6 cells/ml. Cell volume assumed to be 1.4×10^{-9} ml.
[c] Assayed value of S_T is $3.4 \pm 0.4 \times 10^5$/cell, which was rounded up so that $S_T = R_T$.

phosphorylation have a much larger effect on model results and are derived from experimental observations. We set rate constants for Lyn-mediated phosphorylation of β, γ, and Syk so that the binding of Lyn's SH2 domain to the phosphorylated β ITAM raises the phosphorylation rate 3-fold, consistent with the level of increase in activation measured in vitro when Lyn binds to ITAM phosphopeptides (10, 11). In the model the rate constants for ITAM phosphorylation are for converting an unphosphorylated ITAM to a phosphorylated ITAM that acts as a high affinity docking site. The rate constant for γ ITAM phosphorylation is taken to be 30 times lower than the rate constant for β ITAM phosphorylation because Syk binding requires double phosphorylation of the γ ITAM, and both biochemical and structural evidence indicates a strong preference by Lyn to phosphorylate one of the two γ ITAM tyrosines, the N-terminal tyrosine, suggesting that double phosphorylation is considerably slower than phosphorylation of the first tyrosine (48, 49). The magnitude of the difference in β and γ ITAM phosphorylation rates, i.e., the factor of 30, was determined by requiring that the removal of the high affinity Lyn-receptor interaction has a negative effect on the total amount of Syk autophosphorylation, i.e., that the β ITAM acts as an amplifier of signaling (30). The underlying analysis is presented below (see *The β ITAM can act as an amplifier or inhibitor*).

Syk is phosphorylated in the model by either Lyn or Syk through transphosphorylation (19, 21, 23, 50). In the model Lyn phosphorylates Syk tyrosines located in the linker region, while Syk phosphorylates the activation loop tyrosines (21, 23). Although Lyn may be responsible in vivo for a small portion of the Syk activation loop phosphorylation, full Syk activation is achieved only when kinase-active Syk is available (19, 21). In the current model linker region phosphorylation is used only as a marker and has no effect on Syk activity or binding properties. Recent studies indicate that the four linker region tyrosines have distinct and possibly competing effects that are difficult to lump together (21, 23, 24). The model can be augmented to include such effects as further information becomes available. Activation loop phosphorylation serves as a marker of Syk activation for downstream events and produces a 2-fold increase in Syk activity (24).

The last reaction class in Fig. 2 indicates that phosphorylated units that are not protected through association with an SH2 domain can be dephosphorylated, with a common rate constant, d, which we call the intrinsic rate constant for dephosphorylation. Dephosphorylation is blocked when an SH2 domain is associated with the phosphorylated site (29). The intrinsic dephosphorylation rate is fit together with the rate constants for Lyn and Syk dissociating from phosphorylated ITAMs to match experimentally observed dephosphorylation rates (51), as described below in *Interpretation of dephosphorylation kinetics*. Good agreement is obtained only when d is much faster than the observed dephosphorylation rate, which is required for dephosphorylation to compete with kinase binding. The rate of kinase dissociation from phosphorylated receptors thus effectively controls the observed rate of dephosphorylation in the model.

Model summary

The model we have described consists of a reaction network with 354 distinct chemical species (Fig. 1) and the 3680 chemical reactions (Fig. 2) that connect them. The components and the wiring that connects them are based on a large number of biochemical experiments with several different cell types that have been reported in the literature and discussed above. A comparatively small number of rate constants and concentrations (Table I) parameterize the model, and their

numerical values are specific to RBL cells. We have written a computer program to generate the states and reaction network from the components and rules given above. The program was validated both against a human-generated reaction list and a list produced by a second program using a different algorithm. The network along with the rate parameters and initial concentrations are passed to a second program that generates and solves a set of 354 differential equations for the concentration of each chemical species as a function of time using standard methods (52). To compare simulation results with experiments, we add up the concentrations of species with a particular characteristic, e.g., phosphorylated γ ITAM. The programs that implement our model are freely available at our web site: http://cellsignaling.lanl.gov.

Results

We present three types of results: tests of mechanistic assumptions, estimation of unknown parameters, and additional tests to determine whether model predictions based on the estimated parameters are quantitatively consistent with available data. The results are interrelated. For example, the analysis that addresses the mechanisms underlying the amplification function of the β ITAM is also essential for estimating a key parameter, the rate at which Lyn transphosphorylates both tyrosines in a γ ITAM. Furthermore, all parameter values, estimated from multiple experiments, are used in the tests for consistency of model predictions with the data. The following presentation of the interrelated results is organized in terms of different types of experiments.

In the first three subsections we show that for the parameter estimates summarized in Table I, the model is quantitatively consistent with RBL cell data on the kinetics of phosphorylation of receptor subunits and Syk, dose-response relations, kinetics of dephosphorylation of receptor subunits, and differences between the γ and β subunits in all three of these types of experiments.

The remaining subsections use the model to predict changes in system behavior in experiments in which particular system parameters are altered. We show, by simulating experiments with three ligands that have different dissociation rate constants, that the model predicts behavior indicative of kinetic proofreading, consistent with the observations of Torigoe et al. (44). The other perturbations we consider involve changes in the intracellular content or activity of the interacting molecules. In these cases our results serve two functions. One is to pin down parameter values that characterize the RBL cell system, since we find that certain changes in parameter values will change the predicted behavior so that it is no longer consistent with RBL cell data. The second function of predicting cell behavior when a parameter is altered is to identify experiments, using appropriate transfectants, to test mechanistic assumptions of the model (e.g., the assumption that Syk autophosphorylation is intermolecular) or to determine conditions consistent with experimentally observed behavior (e.g., signal amplification or, potentially, signal inhibition by the β ITAM).

Consistency of the model with phosphorylation kinetics

As a first test of the model, we examine the kinetics of receptor aggregation and tyrosine phosphorylation (Fig. 3) in RBL cells stimulated with covalently linked dimers of IgE (28). A feature of dimer-induced receptor phosphorylation is that it persists for a long period (at least an hour) rather than rising, going through a maximum, and then decreasing rapidly, as is seen with multivalent Ags (27). At a 1.6 nM dimer concentration, receptor aggregation reaches half of its maximum value at ~25 min and is still increasing after 1 h (Fig. 3*a*). In contrast, the levels of receptor ITAM phosphorylation plateau at much earlier times in both the experiments and the model simulations (Fig. 3*b*). The times to reach half-maximum value in the model under these conditions are 5 min for β phosphorylation and 9 min for γ phosphorylation, values that are comparable to the ~10 min time scale observed experimentally.

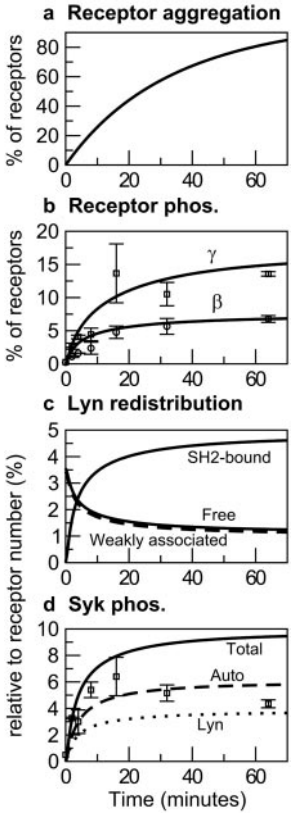

FIGURE 3. Simulated and observed kinetics of phosphorylation and other early signaling events following incubation of RBL cells with 1.6 nM IgE dimer. Curves show model predictions. Data points in *b* and *d* are from densitometric measurements of phosphorylation in a single representative experiment, plotted previously in Fig. 4 of Ref. 28. For quantitative comparison with model predictions, all data were scaled using a common scaling factor, so that predicted and observed levels of β phosphorylation matched at 64 min. Other scaling choices are possible, and there is no obvious best choice, because the factor needed to convert from OD to receptor fraction varies from experiment to experiment and is not measured. *a*, Predicted percentage of receptors in aggregates. *b*, Percentage of receptors phosphorylated on β or γ ITAMs. *c*, Predicted amount of Lyn per receptor in each of its three possible states: free, weakly associated with unphosphorylated FcεRIβ, or bound through its SH2 domain to the phosphorylated β ITAM. The total amount of available Lyn is 7% the number of receptors. *d*, Amount of Syk per receptor phosphorylated by Lyn (dotted line), phosphorylated by Syk (dashed line), and phosphorylated by Lyn or Syk (solid line).

The kinetics of receptor and Syk phosphorylation in the model are determined by two primary factors. First, ligand-receptor binding is the rate-limiting step, so that except at early times (<1 min) there is a quasi-equilibrium between the number of aggregates and all downstream events. In other words, the amount of receptor or Syk phosphorylation at 10 min is nearly identical with the amount that would be observed at a steady state with the same total number of aggregates. Second, the initiating kinase Lyn is in limited supply, which leads to a saturation of receptor phosphorylation at a relatively low level of aggregation. The current results indicate that when Lyn is limiting, early saturation occurs in β and γ ITAM phosphorylation, as well as Syk phosphorylation. In addition, the model predicts that when the amount of Lyn is increased, phosphorylation increases, and saturation of phosphorylation is shifted

to later times (simulations not shown). The sensitivity of the model to Lyn concentration and the agreement between experiments and the model predictions at low, but not high, Lyn concentrations provide strong additional support for the contention that Lyn is limiting in RBL cells.

Fig. 3*b* shows that the level of γ phosphorylation exceeds that of β phosphorylation by ~2-fold, in agreement with both previous measurements (28) and current data (see below). A γ ITAM tyrosine that becomes phosphorylated has a longer lifetime than a β phosphotyrosine because the concentration of Syk, which binds to the γ ITAM, is much higher than that of Lyn, which binds to the β ITAM. Protection thus acts as a mechanism to amplify γ phosphorylation in relation to β phosphorylation and more than compensates for the slower rate at which Lyn phosphorylates γ compared with β. This amplification can be quantified by the ratio of γ to β phosphorylation, which is discussed more in the next section. The increase in this ratio with time and with increasing aggregation causes the shift in the plateau of γ phosphorylation to longer times.

The time course in Fig. 3*c* shows a rapid redistribution of Lyn, which upon aggregation becomes much more tightly associated with the receptor through binding of its SH2 domain to the phosphorylated β ITAM. At maximum receptor aggregation, ~80% of available Lyn is bound through its SH2 domain to β, which amounts to ~5% of receptors with SH2-bound Lyn. The model predicts an ~2-fold increase in the amount of Lyn associated with receptor upon stimulation. Chemical cross-linking experiments have indicated an ~3-fold increase in Lyn association upon stimulation (11).

Finally, Fig. 3*d* shows that the predicted Lyn- and Syk-mediated phosphorylations of Syk have similar kinetics and magnitude. It is unclear at present whether the catalytic activity of unphosphorylated Syk bound to the γ ITAM is sufficient to transphosphorylate an adjacent Syk molecule (24), as assumed by the model, or whether Syk must first be activated by Lyn (19). In any event, the predicted time course of total Syk phosphorylation captures the short time behavior of the experimentally determined time course. At long times Syk phosphorylation drops off, while the predicted level plateaus. Since the model does not include components that interact with phosphorylated Syk, such as Cbl (53), discrepancies at long times are not surprising.

Consistency of the model with dose-response curves

Fig. 4 shows the results of both simulations and experiments in which we have stimulated RBL cells with varying concentrations of covalently linked IgE dimers for 10 min. There is good agreement between the simulated and experimental results for receptor and Syk phosphorylation (Fig. 4, *b* and *d*). The model predicts that phosphorylation in response to aggregation is shifted to lower ligand concentrations than aggregation, and that Syk phosphorylation is shifted farther than receptor phosphorylation. For example, receptor phosphorylation at 2 nM is ~65% of the maximum at higher ligand concentrations, while Syk phosphorylation is ~85% of its maximum value. The experimental results also support this trend. As was the case for the kinetics, simulations with Lyn in excess shift the response to higher aggregate concentrations and fail to achieve reasonable agreement with experiments (simulations not shown).

Fig. 4*c* shows the ratio of γ-phosphorylated receptors to β-phosphorylated receptors, which is determined independently at each concentration. The experimental ratio is consistently higher than the simulated result, although the discrepancy is minimal at high ligand concentrations. In all cases the γ/β ratio is significantly >1, which arises in the model from the fact that there is ~10-fold more

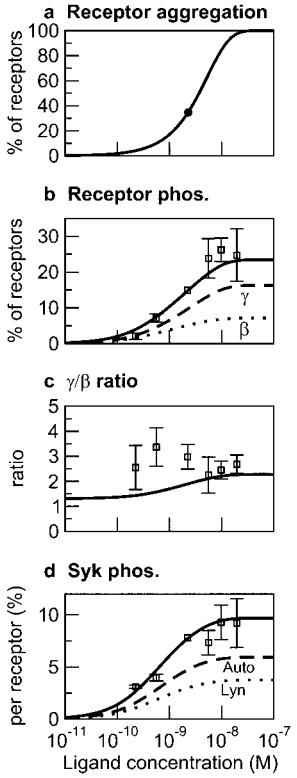

FIGURE 4. Comparison between simulated and experimental dose-response curves for receptor and Syk phosphorylation at 10 min as a function of the initial IgE dimer concentration. The experimental data represent the results of at least three independent experiments in which RBL cells were exposed to the indicated concentrations of IgE dimer. □, mean values. Error bars indicate SEs. Since the level of phosphorylation for each experiment was determined relative to the phosphorylation at 2 nM, no error bars are shown for this point. The absolute level of phosphorylation is not determined in the experiments; therefore, we have scaled the experimental data so that the predicted and measured values match at 2 nM. *a*, Percentage of receptors in aggregates. *b*, Percentage of receptors phosphorylated on β ITAMs (dotted line), γ ITAMs (dashed line), and total (solid line). *c*, Ratio of the number of γ dimers phosphorylated to the number of β subunits phosphorylated. *d*, Amount of Syk per receptor phosphorylated by Lyn (dotted line), phosphorylated by Syk (dashed line), and phosphorylated by Lyn or Syk (solid line).

Syk than Lyn available to bind and protect phosphotyrosines. The model predicts that the γ/β ratio increases with increasing ligand concentration because the amount of free Lyn available to rebind and protect β phosphotyrosines decreases as the number of aggregates increases, while the amount of free Syk is affected to a much smaller extent.

Interpretation of dephosphorylation kinetics

Mao and Metzger (51) measured the rates of dephosphorylation for the β and γ ITAMs in RBL cells by adding an excess of monovalent hapten to break up aggregates induced by DNP-BSA ligand binding to anti-DNP IgE. We simulated this experiment with our model using the forward rate constants for the IgE dimer while setting the reverse rate constants k_{-1} and k_{-2} to 0.5 s^{-1}. Setting the ligand concentration to 1.7 nM for 2 min induces ~5% of the receptors to form dimers. Hapten addition is then modeled by setting the ligand forward rate constants to zero, allowing the dimers to break up, but not re-form. We fit three model parameters, the intrinsic dephosphorylation rate constant, *d*, the rate constant for Lyn dissociating from the phosphorylated β ITAM, k^*_{-L}, and a

common rate constant for activated or nonactivated Syk dissociating from the phosphorylated γ ITAM, $k_{-S} = k^*_{-S}$, to match the observed dephosphorylation rates (51) of 0.12 s^{-1} for β and 0.06 s^{-1} for γ. The results of the fit are shown in Fig. 5. Good agreement is obtained only when d is much higher than the observed rate of dephosphorylation, d_{obs}. This result can be explained by a simple three-state model of dephosphorylation,

$$\text{R-P-E} \underset{k_{+E}E}{\overset{k_{-E}}{\rightleftharpoons}} \text{R-P} \xrightarrow{d} \text{R},$$

where R is receptor, R-P is phosphorylated receptor, and R-P-E is enzyme-bound phosphorylated receptor. At steady state

$$d_{obs} = \frac{k_{-E}}{1 + k_{+E}E/d} \quad (1)$$

and thus the observed dephosphorylation rate is limited by the kinase dissociation rate, k_{-E}. In addition, d_{obs} will be slower than k_{-E} if d cannot compete with the rate of kinase binding, $k_{+E}E$. In the current model the maximum rate of kinase binding, $k_{+E}E$, is 1.4 s^{-1} for Lyn and 24 s^{-1} for Syk. The thin dashed lines in Fig. 5 show that setting d at a value of 0.12 s^{-1} (the experimentally observed rate of β dephosphorylation) results in very slow dephosphorylation rates in the model, as expected from Equation 1. In our fits the equilibrium constant, $K_E = k_{+E}/k_{-E}$, was fixed, which places the lower limit on d of $d_{obs}K_EE$ or ~11 s^{-1} for Syk. The fit shown in Fig. 5 was obtained by setting $d = 20$ s^{-1} and adjusting the kinase dissociation rates to match d_{obs} from the experiment (51). For these parameters R-P has about an equal chance of binding Syk or being dephosphorylated, and dephosphorylation occurs at about half the rate of Syk dissociation. Changing the enzyme concentration affects this balance and changes both the observed rate of dephosphorylation and the level of phosphorylation achieved at steady state, as we investigate below. Fig. 5 shows that reducing either of the kinase concentrations 10-fold increases the apparent rate of dephosphorylation, but not to the level of either the aggregate breakup rate (1 s^{-1}) or the intrinsic dephosphorylation rate (20 s^{-1}). Thus, the effects of protection can be expected to persist even at relatively low kinase concentrations.

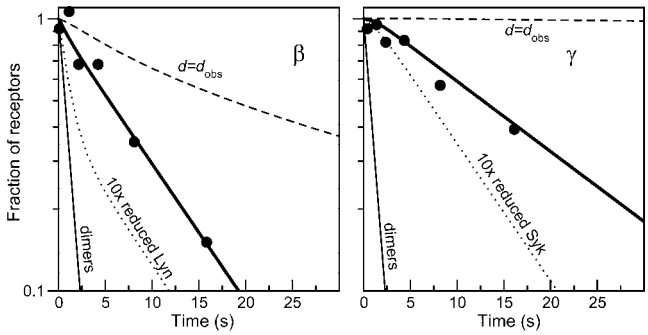

FIGURE 5. Dephosphorylation of FcεRI following disaggregation of receptors. Predicted (thick solid lines) and measured (●) (51) fractions of receptors that remain phosphorylated after the addition of monovalent hapten to break up receptor aggregates. The thin dashed lines show the much slower dephosphorylation that results when the intrinsic dephosphorylation rate in the model, d, is set at the experimentally observed dephosphorylation rate, d_{obs}. The thin dotted lines show the increased rate of dephosphorylation when the amount of Lyn or Syk is reduced 10-fold. The thin solid lines show the fraction of receptors remaining in dimers, which break up at a rate of 1 s^{-1} in these simulations.

Concentration of Syk available for receptor binding

Changing the Syk concentration in the model can affect early signaling events in two primary ways: increasing the concentration of Syk SH2 domains can lead to increased γ ITAM phosphorylation through protection of ITAM tyrosines from dephosphorylation (as described above), and increasing the concentration of the Syk kinase domain can lead to increased Syk activation through autophosphorylation. The first effect is demonstrated in Fig. 6*a*, which shows the increase in the ratio of γ to β phosphorylation as the Syk concentration in the model is increased. The γ/β phosphorylation ratio measured experimentally at the corresponding ligand concentration lies in the range of 2–3, which occurs in the model at a Syk concentration where the total number of Syk molecules available to interact with phosphorylated receptors is close to the total number of receptors. For the model to be consistent with the data, the number of Syk molecules available to receptors must be close to the assayed number of Syk molecules per cell, in contrast to the situation with Lyn, where the availability of Lyn within the receptor compartment appears to be much lower than its overall concentration within the cell (3). Because bound Syk protects γ ITAM phosphotyrosines from phosphatases, the abundance of available Syk has the effect of increasing double phosphorylation of the γ ITAM to a much higher level than can be maintained through the action of Lyn alone.

The results of the model for receptor phosphorylation can also be compared with the experimental results of Scharenberg et al. (54), who observed an increase in receptor phosphorylation of Ag-stimulated RBL cells transfected with porcine Syk or truncated

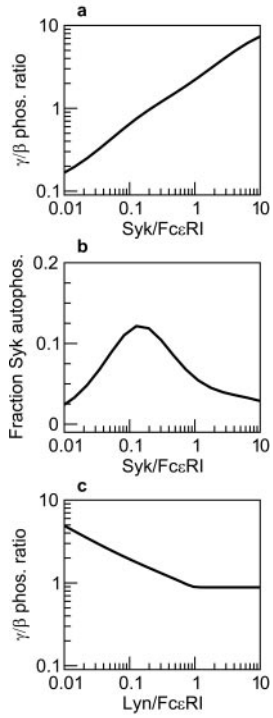

FIGURE 6. Predicted receptor phosphorylation ratio and fraction of Syk autophosphorylated as a function of the number of available Syk or Lyn molecules per cell. Phosphorylation is simulated at 10 min following addition of 10 nM IgE dimer. *a*, Ratio of γ to β receptor subunit phosphorylation, as a function of the Syk concentration, with the amount of Lyn fixed at 2.8×10^4/cell. *b*, Fraction of Syk autophosphorylated, as a function of the Syk concentration. *c*, Ratio of γ to β receptor subunit phosphorylation, as a function of the Lyn concentration with the amount of Syk fixed at 4×10^5/cell.

porcine Syk protein that contained only the Syk tandem SH2 domains compared with Ag-stimulated untransfected RBL cells. The fact that increased phosphorylation was observed when only the truncated Syk was expressed was taken as evidence that the increase in phosphorylation could not be attributed to direct receptor phosphorylation by Syk, but, rather, to protection of phosphotyrosines from dephosphorylation by the binding of Syk SH2 domains. The model results shown in Fig. 6*a* strongly support this interpretation (since Syk does not phosphorylate the receptor in the model) and demonstrate that the predicted dose-response relationship between Syk concentration and receptor ITAM phosphorylation arising from this mechanism is maintained over a range of Syk concentrations spanning at least three orders of magnitude. Note that the predicted change in the γ/β ratio shown in Fig. 6*a* is entirely the result of increasing the γ ITAM phosphorylation; the level of β phosphorylation is unaffected by the Syk concentration because in the model Syk binds only to the phosphorylated γ ITAM. Scharenberg et al. (54) also observed an increase in phosphorylation of the β ITAMs upon overexpression of Syk, which suggests that at very high Syk concentrations, Syk SH2 domains may bind and protect the β ITAM phosphotyrosines as well.

Fig. 6*b* shows that the efficiency of Syk activation, measured as the fraction of Syk molecules that is activated upon stimulation, peaks at ~0.12, when the number of Syk molecules is ~10% the number of receptors. The value when the number of Syk molecules is equal to the number of receptors is ~0.05, consistent with our experimental measurement of 0.06 for RBL cell stimulation with covalently cross-linked IgE dimers.

Effect of Lyn concentration on the γ/β phosphorylation ratio

In contrast to variation of the γ/β phosphorylation ratio with Syk concentration (Fig. 6*a*), increasing the Lyn concentration decreases the predicted γ/β phosphorylation ratio over a broad concentration range (Fig. 6*c*). The experimentally observed ratio is consistent with the concentration of Lyn available to receptors being ~5–10% of the number of receptors, as estimated previously based on the kinetics of total receptor phosphorylation (3). The change in the γ/β phosphorylation ratio with Syk concentration resulted solely from Syk's role in protecting γ-phoshotyrosines from dephosphorylation. Dependence of the γ/β phosphorylation ratio on the Lyn concentration is complicated by the fact that Lyn affects both β and γ phosphorylation and the fact that Lyn has two types of interaction with the β subunit.

Mechanism of Syk autophosphorylation

In the model we have presented, the mechanism for Syk autophosphorylation is transphosphorylation. A Syk molecule bound to one receptor in an aggregate phosphorylates a Syk bound to the other receptor (Fig. 2). This hypothesis seems reasonable because transphosphorylation has been established as the primary mechanism of tyrosine phosphorylation of the epidermal growth factor receptor and other receptor kinases (55) and FcεRI (15). On the other hand, although Lyn acts on receptor ITAMs by transphosphorylation, the juxtaposition of two Lyn molecules in a receptor aggregate is not required for Lyn to be active (4). The analysis in Ref. 4 depended on the experimental observation of a linear relation between the amounts of Lyn in a series of stable transfectants and the extent of ITAM phosphorylation, i.e., phosphorylation was simply proportional to the amount of Lyn. The relation would have been quadratic, i.e., phosphorylation would have been proportional to the square of the concentration of available Lyn, if juxtaposition of two Lyns were required. With appropriate transfectants, similar methods could be used to test the hypothesis that phosphorylation of Syk tyrosines by Syk is transphosphorylation. Fig. 7 shows what the current model predicts for experiments with transfectants having different amounts of Lyn and Syk. Syk autophosphorylation would depend quadratically on the concentrations of both Lyn (Fig. 7*a*) and Syk (Fig. 7*b*).

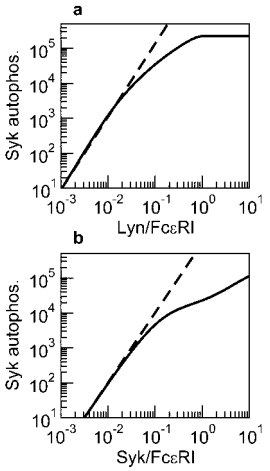

FIGURE 7. Predicted Syk autophosphorylation as a function of the number of available Syk or Lyn molecules per cell. Phosphorylation is simulated at 10 min following addition of 10 nM IgE dimer. The number of autophosphorylated Syk molecules per cell (solid lines) is plotted as a function of the concentrations of Lyn (*a*) and Syk (*b*). Power law fits at low kinase concentrations (dashed lines) give exponents of 2.1 for Lyn and 2.0 for Syk.

How would alternative findings be interpreted? If Syk autophosphorylation varies linearly with the cellular content of Syk, we would have to consider a model in which the kinase domain of a Syk molecule phosphorylates tyrosines in the activation loop of the same molecule. If Syk autophosphorylation varies quadratically with the concentration of Syk but linearly with the concentration of Lyn, we would consider a model in which, when Lyn phosphorylates a γ dimer, two Syks can bind to the dimer. As discussed earlier, we assumed for steric reasons that only one Syk can bind to the γ dimer, but this assumption can be modified if there is evidence to the contrary. A linear dependence of the level of phosphorylation of specific Syk tyrosines on the concentration of Lyn could also indicate that the residues examined are phosphorylated primarily by Lyn, not Syk.

Variation of aggregate lifetime: evidence for kinetic proofreading

A number of recent experimental and theoretical models have shown that one major criterion by which signaling pathways discriminate between different ligands is the lifetime of the ligand-receptor bond (44, 56–64). The basic idea behind this kinetic proofreading, in analogy to similar mechanisms in biosynthetic pathways (65), is that rapidly, dissociating ligands are less effective than slowly dissociating ligands in stimulating downstream signaling events that require completion of a sequence of biochemical reactions while the supramolecular complex of ligand, receptors, and associated signaling molecules remains intact. A key assumption is that the entire complex dissociates, and biochemical modifications are reversed rapidly once the ligand dissociates. Thus, the ligand-receptor bond serves as a timer for downstream signaling events, and ligands with short lifetimes will be ineffective at triggering events that require longer times to commence.

We tested whether our model exhibits the basic features of kinetic proofreading by comparing the levels of receptor and Syk phosphorylation achieved by three different hypothetical bivalent

ligands with the same forward rate constants (k_{+1} and k_{+2}), but different dissociation rate constants (k_{-1} and k_{-2}). To equalize the comparison, the levels of phosphorylation are plotted as a function of the number of aggregates formed. The *top panel* of Fig. 8 shows that for each 10-fold increase in the ligand dissociation rate constants, the ligand concentration must be raised ~100-fold to maintain the same level of aggregation. As the ligand affinity decreases, the maximum number of aggregates that may be formed also decreases, restricting the range of comparison. The results shown in the three *bottom panels* of Fig. 8 show that proximal events, represented by β and γ phosphorylation, are affected much less by the change in ligand-receptor lifetime than Syk autophosphorylation, which is the furthest downstream event in our model. The effect of kinetic proofreading on Syk activation is particularly dramatic at low ligand concentrations; there is a >100-fold change in the level of activation going from the medium affinity ligand to the low affinity ligand.

Interestingly, the extent of kinetic proofreading is predicted to decrease as the ligand concentration increases, and there is even a cross-over for γ phosphorylation at high concentrations. This effect can be explained as follows. The level of phosphorylation can be enhanced by increasing the mobility of kinases. For example, increasing the dissociation rate constant for constitutively associated Lyn in the model (k_{-L}) actually increases the levels of β and γ phosphorylation at high aggregate concentrations, because each Lyn can phosphorylate more than one receptor. An analogous phenomenon, known as serial engagement (66, 67), is observed in T cell signaling in which a single MHC peptide can stimulate a substantial number of TCRs. Increasing the ligand-receptor dissociation rate effectively increases the mobility of kinases associated with the receptor. The time for an uncomplexed receptor to join an aggregate decreases as the ligand concentration is increased, and thus the enhancement of phosphorylation from increased kinase mobility competes more effectively with kinetic proofreading at the highest ligand concentrations. This mechanism demonstrates an exception to the standard assumption in kinetic proofreading models that dissociation of the ligand leads to the complete reversal of all receptor modifications made during the lifetime of the aggregate.

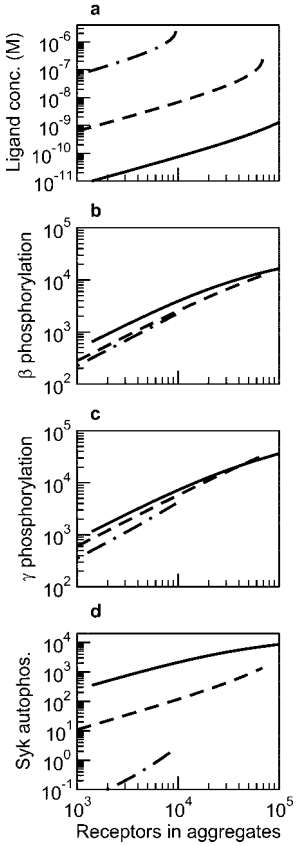

FIGURE 8. Simulation of kinetic proofreading through variation of the rate constant for ligand dissociation. The values shown are obtained at steady state. The forward rate constants are fixed at $k_{+1} = 10^6\ M^{-1}\ s^{-1}$ and $k_{+2}R_T = 0.5\ s^{-1}$, while the reverse rate constants, $k_{-1} = k_{-2}$, are set at 0.05 s^{-1} (solid lines), 0.5 s^{-1} (dashed lines), and 5 s^{-1} (dash-dot lines). The horizontal axis indicates levels of FcεRI aggregation, given as the number of receptors per cell in aggregates. *a*, Ligand concentrations required to achieve specified levels of receptor aggregation. *b*, Number of receptors per cell phosphorylated on β. *c*, Number of receptors per cell phosphorylated on γ. *d*, Number of autophosphorylated Syk molecules per cell.

The β ITAM can act as an amplifier or inhibitor

The β subunit has been called an amplifier of FcεRI signaling both because $\alpha\beta\gamma_2$ receptors produce a much stronger signal in response to stimulation than $\alpha\gamma_2$ receptors (30) and because expression of the β subunit greatly increases receptor expression at the cell surface (68). One reason why the β subunit might act as a signal amplifier is the specific high affinity interaction between Lyn's SH2 domain and the phosphorylated β ITAM (42).

Two studies have directly addressed the effect of this interaction. Lin et al. (30) observed an ~7-fold reduction in γ ITAM phosphorylation when the three β ITAM tyrosines were mutated to phenylalanine in receptors transfected into NIH-3T3 cells. By comparison, the reduction in γ ITAM phosphorylation was ~20-fold when the entire β subunit was removed from the receptor (30). One difficulty in assessing the importance of the high affinity interaction in this study is the possibility that the low affinity interaction of Lyn with the receptor is also affected by changes in the β ITAM. Another approach was taken by Honda et al. (69), who transfected various Lyn constructs lacking the C-terminal region into RBL cells and used overexpression of C-terminal Src kinase binding protein to suppress the activity of endogenous Lyn. They found that deletion of Lyn's SH2 domain produced only a modest decrease in receptor phosphorylation, but nearly eliminated Syk phosphorylation and other downstream events. The authors attributed these results to a form of kinetic proofreading arising from the disruption of the high affinity Lyn-receptor interaction. According to this hypothesis, the low affinity interaction was sufficient to produce a significant level of receptor phosphorylation, but later events were disrupted by the short lifetime of the Lyn-receptor interaction.

Fig. 9 shows the effect of removing the high affinity Lyn-receptor interaction from the model on γ ITAM and Syk phosphorylation. This is accomplished by simply setting the rate constant for β phosphorylation by Lyn ($p_{L\beta}$) to zero. The results are reported in terms of the gain produced by including the high affinity interaction. The gain is defined as the ratio of the phosphorylation when the ITAM is present to the phosphorylation if the ITAM is effectively absent. As observed by Honda et al. (69), the gain in downstream Syk autophosphorylation is greater than that in γ phosphorylation at all ligand concentrations (Fig. 9*a*). The magnitude of both gains, however, exhibits a strong concentration dependence, and at the highest ligand concentrations the high affinity interaction acts as a slight inhibitor of γ phosphorylation. These results cannot be explained by kinetic proofreading alone. The amount of downstream phosphorylation induced by Lyn may be written as the product of two terms: the average number of Lyn molecules per aggregate and the average efficiency of each Lyn in an aggregate at producing the event, e.g., the amount of Syk autophosphorylation divided by the amount of Lyn in aggregates. The gain in Lyn recruitment plotted in Fig. 9*a* shows that most of the gain in Syk autophosphorylation and its strong concentration dependence can be attributed

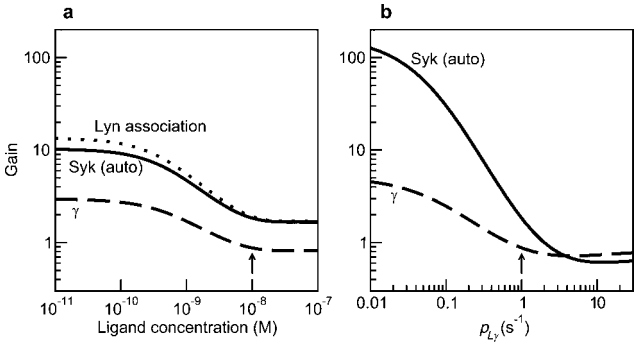

FIGURE 9. Simulated effect of removing the high affinity interaction between Lyn and the phosphorylated β ITAM. The reported gain is the amount of phosphorylation with the β ITAM intact divided by the amount of phosphorylation in the absence of a functional β ITAM, which is modeled by setting the rate constant for β ITAM phosphorylation, $p_{L\beta}$, at zero. Gains are reported for Syk autophosphorylation (solid line), γ phosphorylation (dashed line), and the amount of Lyn associated with aggregates (dotted line). *a*, Gains as a function of the ligand concentration. *b*, Gains as a function of the rate at which Lyn transphosphorylates the γ ITAM. The two parameters in the model that govern this rate are $p_{L\gamma}$, for constitutively bound Lyn and $p^*_{L\gamma}$ for Lyn bound to the β ITAM. They are varied simultaneously keeping $p^*_{L\gamma} = 3p_{L\gamma}$. The arrow in *a* indicates the concentration used in *b*, while the arrow in *b* marks the value of $p_{L\gamma}$ used in *a*.

to the enhanced recruitment of Lyn into aggregates through the high affinity Lyn-receptor interaction. The fact that the gain in Syk autophosphorylation and that in Lyn association match closely demonstrates that the relative efficiency for the production of autophosphorylated Syk is nearly the same for the high and low affinity interactions of Lyn with β. As was the case with ligand-receptor lifetimes, there is a competition between the effect of kinetic proofreading, which favors the high affinity interaction, and serial engagement, which favors the low affinity interaction. For the proximal event, γ phosphorylation, serial engagement dominates, while for Syk autophosphorylation there is a nearly equal balance of the two effects. It thus appears that for the current model parameters the predominant effect of the high affinity interaction is not kinetic proofreading, but selective recruitment of Lyn to aggregates.

This balance between kinetic proofreading and serial engagement in the Lyn-receptor interaction can be shifted by varying the rate constants for γ phosphorylation by Lyn, $p_{L\gamma}$ and $p^*_{L\gamma}$, as shown in Fig. 9*b*. Changing these parameters changes the length of time Lyn must stay associated with the receptor to propagate the signal downstream, but does not affect the Lyn-receptor interaction. Decreasing the phosphorylation rate constants increases the effect of kinetic proofreading, leading to larger gains in both γ phosphorylation and Syk autophosphorylation. For moderate increases in the rate constants, on the other hand, serial engagement becomes dominant, and the high affinity interaction becomes an inhibitor of both γ and Syk phosphorylation.

Discussion

We developed a detailed kinetic model for the early events in FcεRI-mediated signaling, from receptor-ligand binding through the autophosphorylation of Syk. We applied the model to extract quantitative and qualitative information from new and published data and to identify additional experiments that can be used to test the model and improve estimates of key parameters.

The model is detailed in the sense that it describes events at the molecular level, including ligand-induced aggregation of receptors (FcεRI), association of receptor subunits (β and γ) with two protein tyrosine kinases (Lyn and Syk), and phosphorylation and dephosphorylation of specified sets of tyrosines on β, γ, and Syk. The model makes predictions as a function of time, ligand concentration, concentrations of signaling components, and potential experimental modifications of the interacting proteins (e.g., removal or impairment of a domain). The last area is particularly important because so much of what we know about signaling pathways comes from genetic manipulation of the components. The model provides a tool for interpreting such experiments and designing new ways to use genetically altered proteins to test ideas about molecular interactions and signaling mechanisms.

The model, with the parameters in Table I, is consistent with a variety of experimental data. Simulations of experiments in which RBL cells were exposed to covalently cross-linked dimers of IgE reproduced the observed kinetics of phosphorylation of receptor subunits over a period of 1 h (Fig. 3). Theoretical and experimental dose-response curves also matched closely (Fig. 4). Model-based simulations also agreed with the observed kinetics of dephosphorylation of the β and γ ITAMs (Fig. 5).

Some of the parameters in Table I were determined directly in previously reported and new experiments. We estimated other parameters based on the fit of model predictions to data. The data impose severe constraints on the parameters. The constraints carry biological information, for example, information about the control of ITAM dephosphorylation and the availability of kinases.

The Lyn and Syk concentrations that are parameters in the model represent the numbers of molecules of Lyn and Syk available to interact with FcεRI. The amount of available Lyn and Syk may be less than the total number per cell. Previously, we analyzed time courses of phosphorylation of FcεRI in RBL cells using a model that included only Lyn and the receptor (3). The analysis led us to propose that the amount of Lyn available to interact with the receptor was considerably less than the total cellular Lyn. Subsequent experiments involving competition for Lyn among different populations of receptor aggregates were consistent with Lyn being limiting (43). Here, using the expanded model, we presented additional evidence that Lyn is limiting. In contrast, we showed here that the amount of Syk available to interact with the receptor is comparable to that of total cellular Syk. We measured the total number of Syk molecules in RBL cells and found that it is close to the measured number of FcεRI. We showed that all or most of that Syk must be available to the receptors for the model to be consistent with differences between β and γ ITAM phosphorylation levels (Figs. 3 and 4) and differences in the rates of β and γ ITAM dephosphorylation (Fig. 5).

With regard to the control of ITAM dephosphorylation, the key parameters are the intrinsic rate constant for dephosphorylation and parameters that characterize protection from dephosphorylation when Lyn binds to a phosphorylated β ITAM or Syk binds to a doubly phosphorylated γ ITAM. Therefore, the concentrations of available Lyn and Syk as well as rate constants for Lyn and Syk association and dissociation can influence the experimentally observed time course of ITAM dephosphorylation. We showed that in the RBL cell system these parameters have a strong effect. The intrinsic rate of dephosphorylation must be 200–300 times faster than the apparent rate to reproduce the dephosphorylation results reported by Mao and Metzger (51). If the intrinsic rate were lower, dephosphorylation would not compete effectively with kinase binding, and little dephosphorylation would be observed (Fig. 5).

Qualitative aspects of signaling can depend sensitively and in nonobvious ways on parameters. Experiments have shown that the β subunit acts to amplify signaling through FcεRI (30). Experiments in RBL cells demonstrate the role of β ITAM phosphorylation in signal amplification (69). We showed, by comparing model predictions in the presence and the absence of β ITAM

phosphorylation, that amplification depends on the rate at which Lyn transphosphorylates the γ ITAM. If transphosphorylation of γ is fast enough for constitutively bound Lyn to phosphorylate γ efficiently, but the high affinity interaction of Lyn with the phosphorylated β ITAM keeps Lyn from dissociating rapidly and moving on to phosphorylate other receptors, then the model predicts that the high affinity interaction will be inhibitory (see Fig. 9*b*). In Table I, the rate at which Lyn transphosphorylates the γ ITAM is set so that the β ITAM is an amplifier of signaling.

We have summarized the utility of the model for quantitative prediction, which depends on accurate estimation of parameters and feeds back, through comparison of model predictions with data, to improve parameter estimates. Another use of a detailed model is to test simplified models, to determine conditions under which a simplified model makes valid predictions as well as conditions when the results may be misleading. We have shown that the cellular responses in the model depend on the lifetime of the ligand-receptor bond in a way that is qualitatively consistent with the predictions of simplified kinetic proofreading models (Fig. 8). Quantitative predictions of the detailed model provide a standard of comparison for predictions from kinetic proofreading models and potentially clarify the biological interpretation of estimated kinetic proofreading parameters.

One function of a mathematical model is to identify new experiments to test biological ideas. A question that remains open is whether autophosphorylation of Syk is intra- or intermolecular. The model postulates that both Lyn and Syk, associated with one FcεRI in an aggregate, can only transphosphorylate Syk associated with a second receptor in the aggregate. Therefore, in the model autophosphorylation of Syk is intermolecular. Based on the analysis of the model, we suggest a quantitative method for distinguishing among models in which autophosphorylation requires only one Syk acting intramolecularly, two Syks associated with a γ dimer on a single receptor, or two Syks associated with distinct receptors in an aggregate.

To date, the model provides a consistent picture of RBL cell signaling induced by IgE dimers without incorporating spatial effects, in particular the role of specialized lipid domains and the redistribution of receptors during signaling (70–74). In the experimental system we have analyzed, phosphorylation of FcεRI and Syk is maintained dynamically, with rapid dephosphorylation balanced by continued phosphorylation for at least 1 h (27, 28). As the simulated removal of the β ITAM demonstrates, even the low affinity constitutive interaction between Lyn and the receptor is sufficient to maintain a substantial level of ITAM phosphorylation (see Fig. 9*a*) following receptor aggregation. It is possible that dimers do not induce the redistribution of Lyn away from receptors and Syk that has been observed when signaling is initiated by multivalent Ag (75).

An alternative model to ours for the initiation of FcεRI signaling is based on the observation that receptor monomers are found primarily outside of lipid rafts, while aggregated receptors and Lyn tend to colocalize within rafts (71). As a result, the effective Lyn concentration for association with receptors increases upon receptor aggregation. Such effects could, in principle, be incorporated into our mathematical model by partitioning the membrane into compartments, selecting transition rates for each component between compartments, and only allowing components within the same compartment to interact. Given the current uncertainties surrounding the characterization of lipid microdomains, however, we leave the investigation of such a model to future work.

In the model only Lyn phosphorylates receptor ITAMs. Recently it has been demonstrated that a second Src kinase, Fyn, associates with FcεRIβ and plays a key role in mast cell degranulation (76). Fyn is recruited to aggregated FcεRI (76), but whether Fyn competes with Lyn for sites on the receptor is unknown. What role, if any, Fyn plays in ITAM phosphorylation also remains to be elucidated.

A detailed model of a cell signaling cascade will always be a work in progress. Analysis of such a model identifies additional experimental measurements and qualitative manipulations needed to distinguish mechanisms and provide accurate quantitative predictions. The experimental results identify points where the model or the parameter estimates must be modified. Ultimately we want sufficient knowledge for quantitative prediction of larger segments of signaling pathways. To have confidence in such predictions, our approach is to proceed stepwise, testing each extension of the model against many different forms of experimental data.

Acknowledgments

J.R.F. thanks Dan Coombs for many helpful discussions.

References

1. Hunter, T. 2000. Signaling: 2000 and beyond. *Cell 100:113.*
2. Ray, L., L. Chong, and N. Gough. 2002. Computational biology. *Science's STKE* http://stke.sciencemag.org/cgi/content/full/sigtrans;2002/148/eg10.
3. Wofsy, C., C. Torigoe, U. M. Kent, H. Metzger, and B. Goldstein. 1997. Exploiting the difference between intrinsic and extrinsic kinases: implications for regulation of signaling by immunoreceptors. *J. Immunol. 159:5984.*
4. Wofsy, C., B. M. Vonakis, H. Metzger, and B. Goldstein. 1999. One Lyn molecule is sufficient to initiate phosphorylation of aggregated high-affinity IgE receptors. *Proc. Natl. Acad. Sci. USA 96:8615.*
5. Goldstein, B., J. R. Faeder, W. S. Hlavacek, M. L. Blinov, A. Redondo, and C. Wofsy. 2002. Modeling the early signaling events mediated by FcεRI. *Mol. Immunol. 38:1213.*
6. Keegan, A. D., and W. E. Paul. 1992. Multichain immune recognition receptors: similarities in structure and signaling pathways. *Immunol. Today 13:63.*
7. Reth, M. 1989. Antigen receptor tail clue. *Nature 338:383.*
8. Cambier, J. C. 1995. Antigen and Fc receptor signaling: the awesome power of the immunoreceptor tyrosine-based activation motif (ITAM). *J. Immunol. 155: 3281.*
9. Kinet, J. P. 1999. The high-affinity IgE receptor (FcεRI): from physiology to pathology. *Annu. Rev. Immunol. 17:931.*
10. Eiseman, E., and J. B. Bolen. 1992. Engagement of the high-affinity IgE receptor activates Src protein-related tyrosine kinases. *Nature 355:78.*
11. Yamashita, T., S. Y. Mao, and H. Metzger. 1994. Aggregation of the high-affinity IgE receptor and enhanced activity of p53/p56^{lyn} protein-tyrosine kinase. *Proc. Natl. Acad. Sci. USA 91:11251.*
12. Jouvin, M. H. E., M. Adamczewski, R. Numerof, O. Letourneur, A. Valle, and J. P. Kinet. 1994. Differential control of the tyrosine kinases Lyn and Syk by the 2 signaling chains of the high-affinity immunoglobulin-E receptor. *J. Biol. Chem. 269:5918.*
13. Vonakis, B. M., H. X. Chen, H. HaleemSmith, and H. Metzger. 1997. The unique domain as the site on Lyn kinase for its constitutive association with the high affinity receptor for IgE. *J. Biol. Chem. 272:24072.*
14. Vonakis, B. M., H. Haleem-Smith, P. Benjamin, and H. Metzger. 2001. Interaction between the unphosphorylated receptor with high affinity for IgE and Lyn kinase. *J. Biol. Chem. 276:1041.*
15. Pribluda, V. S., C. Pribluda, and H. Metzger. 1994. Transphosphorylation as the mechanism by which the high-affinity receptor for IgE is phosphorylated upon aggregation. *Proc. Natl. Acad. Sci. USA 91:11246.*
16. Nishizumi, H., and T. Yamamoto. 1997. Impaired tyrosine phosphorylation and Ca^{2+} mobilization, but not degranulation, in Lyn-deficient bone marrow-derived mast cells. *J. Immunol. 158:2350.*
17. Hutchcroft, J. E., R. L. Geahlen, G. G. Deanin, and J. M. Oliver. 1992. FcεRI-mediated tyrosine phosphorylation and activation of the 72-kDa protein-tyrosine kinase, PTK72, in RBL-2H3 rat-tumor mast cells. *Proc. Natl. Acad. Sci. USA* 89:9107.
18. Benhamou, M., N. J. P. Ryba, H. Kihara, H. Nishikata, and R. P. Siraganian. 1993. Protein-tyrosine kinase p72^{syk} in high-affinity IgE receptor signaling: identification as a component of pp72 and association with the receptor γ-chain after receptor aggregation. *J. Biol. Chem. 268:23318.*
19. El-Hillal, O., T. Kurosaki, H. Yamamura, J. P. Kinet, and A. M. Scharenberg. 1997. Syk kinase activation by a src kinase-initiated activation loop phosphorylation chain reaction. *Proc. Natl. Acad. Sci. USA 94:1919.*
20. Keshvara, L. M., C. Isaacson, M. L. Harrison, and R. L. Geahlen. 1997. Syk activation and dissociation from the B-cell antigen receptor is mediated by phosphorylation of tyrosine 130. *J. Biol. Chem. 272:10377.*
21. Keshvara, L. M., C. C. Isaacson, T. M. Yankee, R. Sarac, M. L. Harrison, and R. L. Geahlen. 1998. Syk- and Lyn-dependent phosphorylation of Syk on multiple tyrosines following B cell activation includes a site that negatively regulates signaling. *J. Immunol. 161:5276.*
22. Siraganian, R. P., J. Zhang, K. Suzuki, and K. Sada. 2002. Protein tyrosine kinase Syk in mast cell signaling. *Mol. Immunol. 38:1229.*

23. Hong, J. J., T. M. Yankee, M. L. Harrison, and R. L. Geahlen. 2002. Regulation of signaling in B cells through the phosphorylation of Syk on linker region tyrosines: a mechanism for negative signaling by the Lyn tyrosine kinase. *J. Biol. Chem. 277:31703.*
24. Zhang, J., M. L. Billingsley, R. L. Kincaid, and R. P. Siraganian. 2000. Phosphorylation of Syk activation loop tyrosines is essential for Syk function: an in vivo study using a specific anti-Syk activation loop phosphotyrosine antibody. *J. Biol. Chem. 275:35442.*
25. Zhang, J., T. Kimura, and R. P. Siraganian. 1998. Mutations in the activation loop tyrosines of protein tyrosine kinase Syk abrogate intracellular signaling but not kinase activity. *J. Immunol. 161:4366.*
26. Segal, D. M., J. D. Taurog, and H. Metzger. 1977. Dimeric immunoglobulin-E serves as a unit signal for mast-cell degranulation. *Proc. Natl. Acad. Sci. USA 74:2993.*
27. Kent, U. M., S. Y. Mao, C. Wofsy, B. Goldstein, S. Ross, and H. Metzger. 1994. Dynamics of signal-transduction after aggregation of cell-surface receptors: studies on the type-I receptor for IgE. *Proc. Natl. Acad. Sci. USA 91:3087.*
28. Wofsy, C., U. M. Kent, S. Y. Mao, H. Metzger, and B. Goldstein. 1995. Kinetics of tyrosine phosphorylation when IgE dimers bind to Fcε receptors on rat basophilic leukemia-cells. *J. Biol. Chem. 270:20264.*
29. Rotin, D., B. Margolis, M. Mohammadi, R. J. Daly, G. Daum, N. Li, E. H. Fischer, W. H. Burgess, A. Ullrich, and J. Schlessinger. 1992. SH2 domains prevent tyrosine dephosphorylation of the EGF receptor: identification of Tyr^{992} as the high-affinity binding-site for SH2 domains of phospholipase C-γ. *EMBO J. 11:559.*
30. Lin, S. Q., C. Cicala, A. M. Scharenberg, and J. P. Kinet. 1996. The FcεRIβ subunit functions as an amplifier of FcεRIγ-mediated cell activation signals. *Cell 85:985.*
31. Péneff, C., M.-P. Lefranc, and P. Dariavach. 2000. Characterisation and specificity of two single-chain Fv antibodies directed to the protein tyrosine kinase Syk. *J. Immunol. Methods 236:105.*
32. Hlavacek, W. S., A. S. Perelson, B. Sulzer, J. Bold, J. Paar, W. Gorman, and R. G. Posner. 1999. Quantifying aggregation of IgE-FcεRI by multivalent antigen. *Biophys. J. 76:2421.*
33. Posner, R. G., B. Lee, D. H. Conrad, D. Holowka, B. Baird, and B. Goldstein. 1992. Aggregation of IgE receptor complexes on rat basophilic leukemia-cells does not change the intrinsic affinity but can alter the kinetics of the ligand IgE interaction. *Biochemistry 31:5350.*
34. Rivera, J., J.-P. Kinet, J. Kim, C. Pucillo, and H. Metzger. 1988. Studies with a monoclonal antibody to the β subunit of the receptor with high affinity for immunoglobulin E. *Mol. Immunol. 25:247.*
35. Amoui, M., P. Draber, and L. Draberova. 1997. Src family-selective tyrosine kinase inhibitor, pp1, inhibits both FceRI- and Thy-1-mediated activation of rat basophilic leukemia cells. *Eur. J. Immunol. 27:1881.*
36. Chen, T., B. Repetto, R. Chizzonite, C. Pullar, C. Burghardt, E. Dharm, Z. Zhao, R. Carroll, P. Nunes, M. Basu, et al. 1996. Interaction of phosphorylated FcεRIγ immunoglobulin receptor tyrosine activation motif-based peptides with dual and single SH2 domains of $p72^{syk}$: assessment of binding parameters and real, time binding kinetics. *J. Biol. Chem. 271:25308.*
37. Gill, S. C., and P. H. von Hippel. 1989. Calculation of protein extinction coefficients from amino-acid sequence data. *Anal. Biochem. 182:319.*
38. Amoui, M., L. Dráberová, P. Tolar, and P. Dráber. 1997. Direct interaction of Syk and Lyn protein tyrosine kinases in rat basophilic leukemia cells activated via type I Fcε receptors. *Eur. J. Immunol. 27:321.*
39. Metzger, H., S. Eglite, H. Haleem-Smith, I. Reischl, and C. Torigoe. 2002. Quantitative aspects of signal transduction by the receptor with high affinity for IgE. *Mol. Immunol. 38:1207.*
40. Nadler, J. S., S. A. Matthews, M. Turner, and J. P. Kinet. 2001. Signal transduction by the high-affinity immunoglobulin E receptor FcεRI: coupling form to function. *Adv. Immunol. 76:325.*
41. Subramanian, K. 1995. *Binding and Functional Effects of Defined Ligands with Monovalent, Bivalent, and Bispecfic IgE in Solution and on the Cell Surface*. Ph.D. thesis, Cornell University, Ithaca, NY.
42. Kihara, H., and R. P. Siraganian. 1994. Src homology-2 domains of Syk and Lyn bind to tyrosine-phosphorylated subunits of the high-affinity IgE receptor. *J. Biol. Chem. 269:22427.*
43. Torigoe, C., B. Goldstein, C. Wofsy, and H. Metzger. 1997. Shuttling of initiating kinase between discrete aggregates of the high affinity receptor for IgE regulates the cellular response. *Proc. Natl. Acad. Sci. USA 94:1372.*
44. Torigoe, C., J. K. Inman, and H. Metzger. 1998. An unusual mechanism for ligand antagonism. *Science 281:568.*
45. Shiue, L., J. Green, O. M. Green, J. L. Karas, J. P. Morgenstern, M. K. Ram, M. K. Taylor, M. J. Zoller, L. D. Zydowsky, J. B. Bolen, et al. 1995. Interaction of $p72^{syk}$ with the γ-subunits and β-subunits of the high-affinity receptor for immunoglobulin-E, FcεRI. *Mol. Cell. Biol. 15:272.*
46. Ottinger, E. A., M. C. Botfield, and S. E. Shoelson. 1998. Tandem SH2 domains confer high specificity in tyrosine kinase signaling. *J. Biol. Chem. 273:729.*
47. Grucza, R. A., K. Futterer, A. C. Chan, and G. Waksman. 1999. Thermodynamic study of the binding of the tandem-SH2 domain of the Syk kinase to a dually phosphorylated ITAM peptide: evidence for two conformers. *Biochemistry 38: 5024.*
48. Pao, L. I., S. A. Famiglietti, and J. C. Cambier. 1998. Asymmetrical phosphorylation and function of immunoreceptor tyrosine-based activation motif tyrosines in B cell antigen receptor signal transduction. *J. Immunol. 160:3305.*
49. Gaul, B. S., M. L. Harrison, R. L. Geahlen, R. K. Burton, and C. B. Post. 2000. Substrate recognition by the Lyn protein-tyrosine kinase: NMR structure of the immunoreceptor tyrosine-based activation motif signaling region of the B cell antigen receptor. *J. Biol. Chem. 275:16174.*
50. Rivera, V. M., and J. S. Brugge. 1995. Clustering of Syk is sufficient to induce tyrosine phosphorylation and release of allergic mediators from rat basophilic leukemia-cells. *Mol. Cell. Biol. 15:1582.*
51. Mao, S. Y., and H. Metzger. 1997. Characterization of protein-tyrosine phosphatases that dephosphorylate the high affinity IgE receptor. *J. Biol. Chem. 272: 14067.*
52. Hindmarsh, A. C. 1983. ODEPACK: a systematized collection of ODE solvers. In *Scientific Computing*. R. S. Stepleman, ed. North-Holland, Amsterdam, p. 55.
53. Ota, Y., and L. E. Samelson. 1997. The product of the proto-oncogene c-cbl: a negative regulator of the Syk tyrosine kinase. *Science 276:418.*
54. Scharenberg, A. M., S. Q. Lin, B. Cuenod, H. Yamamura, and J. P. Kinet. 1995. Reconstitution of interactions between tyrosine kinases and the high-affinity IgE receptor which are controlled by receptor clustering. *EMBO J. 14:3385.*
55. Lemmon, M. A., and J. Schlessinger. 1994. Regulation of signal-transduction and signal diversity by receptor oligomerization. *Trends Biochem. Sci. 19:459.*
56. McKeithan, T. W. 1995. Kinetic proofreading in T-cell receptor signal-transduction. *Proc. Natl. Acad. Sci. USA 92:5042.*
57. Liu, Z. J., H. Haleem-Smith, H. X. Chen, and H. Metzger. 2001. Unexpected signals in a system subject to kinetic proofreading. *Proc. Natl. Acad. Sci. USA 98:7289.*
58. Hlavacek, W. S., A. Redondo, C. Wofsy, and B. Goldstein. 2002. Kinetic proofreading in receptor-mediated transduction of cellular signals: receptor aggregation, partially activated receptors, and cytosolic messengers. *Bull. Math. Biol. 64:887.*
59. Hlavacek, W. S., A. Redondo, H. Metzger, C. Wofsy, and B. Goldstein. 2001. Kinetic proofreading models for cell signaling predict ways to escape kinetic proofreading. *Proc. Natl. Acad. Sci. USA 98:7295.*
60. Germain, R. N. 2001. The T cell receptor for antigen: signaling and ligand discrimination. *J. Biol. Chem. 276:35223.*
61. Coombs, D., A. M. Kalergis, S. G. Nathenson, C. Wofsy, and B. Goldstein. 2002. Activated TCRs remain marked for internalization after dissociation from pMHC. *Nat. Immunol. 3:926.*
62. Rivera, J., R. Arudchandran, C. Gonzalez-Espinosa, T. S. Manetz, and S. Xirasagar. 2001. A perspective: regulation of IgE receptor-mediated mast cell responses by a LAT-organized plasma membrane-localized signaling complex. *Int. Arch. Allergy Immunol. 124:137.*
63. Rosette, C., G. Werlen, M. A. Daniels, P. O. Holman, S. M. Alam, P. J. Travers, N. R. J. Gascoigne, E. Palmer, and S. C. Jameson. 2001. The impact of duration versus extent of TCR occupancy on T cell activation: a revision of the kinetic proofreading model. *Immunity 15:59.*
64. Swain, P. S., and E. D. Siggia. 2002. The role of proofreading in signal transduction specificity. *Biophys. J. 82:2928.*
65. Hopfield, J. J. 1974. Kinetic proofreading: new mechanism for reducing errors in biosynthetic processes requiring high specificity. *Proc. Natl. Acad. Sci. USA 71: 4135.*
66. Valitutti, S., S. Muller, M. Cella, E. Padovan, and A. Lanzavecchia. 1995. Serial triggering of many T-cell receptors by a few peptide-MHC complexes. *Nature 375:148.*
67. Wofsy, C., D. Coombs, and B. Goldstein. 2001. Calculations show substantial serial engagement of T cell receptors. *Biophys. J. 80:606.*
68. Dombrowicz, D., S. Q. Lin, V. Flamand, A. T. Brini, B. H. Koller, and J. P. Kinet. 1998. Allergy-associated FcRβ is a molecular amplifier of IgE- and IgG-mediated in vivo responses. *Immunity 8:517.*
69. Honda, Z. I., T. Suzuki, H. Kono, M. Okada, T. Yamamoto, C. Ra, Y. Morita, and K. Yamamoto. 2000. Sequential requirements of the N-terminal palmitoylation site and SH2 domain of Src family kinases in the initiation and progression of FcεRI signaling. *Mol. Cell. Biol. 20:1759.*
70. Sheets, E. D., D. Holowka, and B. Baird. 1999. Membrane organization in immunoglobulin E receptor signaling. *Curr. Opin. Chem. Biol. 3:95.*
71. Holowka, D., and B. Baird. 2001. FcεRI as a paradigm for a lipid raft-dependent receptor in hematopoietic cells. *Semin. Immunol. 13:99.*
72. Kovarova, M., P. Tolar, R. Arudchandran, L. Draberova, J. Rivera, and P. Draber. 2001. Structure-function analysis of Lyn kinase association with lipid rafts and initiation of early signaling events after Fcε receptor I aggregation. *Mol. Cell. Biol. 21:8318.*
73. Wilson, B. S., J. R. Pfeiffer, and J. M. Oliver. 2000. Observing FcεRI signaling from the inside of the mast cell membrane. *J. Cell Biol. 149:1131.*
74. Wilson, B. S., J. R. Pfeiffer, Z. Surviladze, E. A. Gaudet, and J. M. Oliver. 2001. High resolution mapping of mast cell membranes reveals primary and secondary domains of FcεRI and LAT. *J. Cell Biol. 154:645.*
75. Ortega, E., A. Lara, I. Lee, C. Santana, A. M. Martinez, J. R. Pfeiffer, R. J. Lee, B. S. Wilson, and J. M. Oliver. 1999. Lyn dissociation from phosphorylated FcεRI subunits: a new regulatory step in the FcεRI signaling cascade revealed by studies of FcεRI dimer signaling activity. *J. Immunol. 162:176.*
76. Parravicini, V., M. Gadina, M. Kovarova, S. Odom, C. Gonzalez-Espinosa, Y. Furumoto, S. Saitoh, L. E. Samelson, J. J. O'Shea, and J. Rivera. 2002. Fyn kinase initiates complementary signals required for IgE-dependent mast cell degranulation. *Nat. Immunol. 3:741.*
77. Pribluda, V. S., C. Pribluda, and H. Metzger. 1997. Biochemical evidence that the phosphorylated tyrosines, serines, and threonines on the aggregated high affinity receptor for IgE are in the immunoreceptor tyrosine-based activation motifs. *J. Biol. Chem. 272:11185.*